Jurnal Jamu Indonesia (2026) 11(3): 233–243
https://jamu-journal.ipb.ac.id/index.php/JJI/index

ISSN 2407-7178
eISSN 2407-7763

Research Article
Doi: https://doi.org/10.29244/jji.v11i3.447

Bioassay-Guided and In Silico Identification of α-Amylase Inhibitors from *Abelmoschus esculentus* Fruit

Identifikasi Inhibitor α-Amilase dari Buah *Abelmoschus esculentus* melalui Pendekatan Bioassay-Guided dan In Silico

Christina Astutiningsih*, Syifaur Rohmah, Novy Dwi Susilowati

Sekolah Tinggi Ilmu Farmasi, Yayasan Pharmasi Semarang, Semarang, Central Java 50193, Indonesia

ARTICLE INFO

Article history
Received on: 2025-10-01
Revised on: 2026-01-17
Accepted on: 2026-03-13

Keyword:
Abelmoschus esculentus;
α-amylase inhibitor;
Antidiabetic;
Bioassay-guided;
In silico

Kata kunci:
Abelmoschus esculentus;
Antidiabetes;
Bioassay-guided;
In silico;
Inhibitor α-amilase

ABSTRACT

Diabetes mellitus is a metabolic disorder characterized by persistent hyperglycemia. Inhibition of α-amylase is one therapeutic strategy for controlling postprandial blood glucose levels. This study aimed to identify active compounds responsible for α-amylase inhibitory activity in *Abelmoschus esculentus* fruit using a bioassay-guided and in silico approach. Methanol extract, fractions, and subfractions were evaluated in vitro for α-amylase inhibition. The most active subfraction was characterized by LC–MS and further analyzed by molecular docking and ADMET prediction. Subfraction 2 showed the strongest inhibitory activity, with 74.2634 ± 4.7091% inhibition. LC–MS identified nine compounds, four of which showed favorable binding affinity and interaction patterns with α-amylase: 2-hydroxy-7-methoxycadalene, N-E-coumaroyl tyramine, homovanillic acid, and quercetin. These findings suggest that *A. esculentus* fruit contains bioactive compounds with potential α-amylase inhibitory activity.

ABSTRAK

Diabetes melitus merupakan gangguan metabolik yang ditandai dengan hiperglikemia persisten. Penghambatan α-amilase merupakan salah satu strategi terapi untuk mengendalikan kadar glukosa darah postprandial. Penelitian ini bertujuan mengidentifikasi senyawa aktif yang bertanggung jawab terhadap aktivitas inhibitor α-amilase pada buah *Abelmoschus esculentus* menggunakan pendekatan bioassay-guided dan in silico. Ekstrak metanol, fraksi, dan subfraksi diuji secara in vitro terhadap aktivitas penghambatan α-amilase. Subfraksi paling aktif dikarakterisasi menggunakan LC–MS, kemudian dianalisis melalui molecular docking dan prediksi ADMET. Subfraksi 2 menunjukkan aktivitas penghambatan tertinggi sebesar 74,2634 ± 4,7091%. LC–MS mengidentifikasi sembilan senyawa, dengan empat senyawa menunjukkan afinitas ikatan dan pola interaksi yang baik terhadap α-amilase, yaitu 2-hydroxy-7-methoxycadalene, N-E-coumaroyl tyramine, homovanillic acid, dan quercetin. Hasil ini menunjukkan bahwa buah *A. esculentus* mengandung senyawa bioaktif yang berpotensi sebagai inhibitor α-amilase.

**Corresponding author:*
Christina Astutiningsih (christinaastutiningsih@gmail.com)

Citation: Astutiningsih, C., Rohmah, S., & Susilowati, N. D. (2026). Bioassay-Guided and In Silico Identification of α-Amylase Inhibitors from *Abelmoschus esculentus* Fruit. *Jurnal Jamu Indonesia*, *11*(3), 233–243. https://doi.org/10.29244/jji.v11i3.447

1. INTRODUCTION

Diabetes mellitus is a metabolic disorder associated with disturbances in carbohydrate, lipid, and protein metabolism and is characterized by persistent hyperglycemia caused by insulin deficiency, insulin resistance, or both (Oguntibeju, 2019; Rivas & Nugent, 2021). Type 2 diabetes mellitus is the most common form of diabetes and is closely associated with chronic hyperglycemia and microvascular complications that contribute to increased morbidity and mortality (Ahmad et al., 2025; Ghosh et al., 2025; Młynarska et al., 2025). One therapeutic strategy for controlling postprandial blood glucose is inhibition of carbohydrate-hydrolyzing enzymes, particularly α-amylase and α-glucosidase, which are involved in the breakdown of complex carbohydrates into absorbable sugars in the small intestine (Li et al., 2022).

Synthetic α-amylase inhibitors such as acarbose are used clinically to reduce postprandial hyperglycemia; however, their use may be associated with gastrointestinal side effects, including nausea, diarrhea, vomiting, and flatulence (Dong et al., 2022). These limitations have encouraged the search for alternative enzyme inhibitors from natural sources. *Abelmoschus esculentus* L., commonly known as okra, contains various secondary metabolites, including alkaloids, flavonoids, phenolics, tannins, saponins, and terpenoids, which may contribute to its biological activity (Astutiningsih & Anggraeny, 2023; Ullah et al., 2024). Previous studies have also reported that *A. esculentus* contains polyphenolic compounds such as *p*-coumaric acid, ferulic acid, sinapic acid, catechin, quercetin, and their derivatives (Agregán et al., 2023; Sun & Shahrajabian, 2023).

Several pharmacological activities of *A. esculentus* fruit have been reported, including antioxidant, anti-inflammatory, antimicrobial, antidiabetic, and antiobesity activities (Durazzo et al., 2018; Hafeez et al., 2020; Herowati et al., 2020; Panighel et al., 2022; Shareef et al., 2023; Xiong et al., 2021). Previous work also showed that the ethyl acetate fraction of *A. esculentus* fruit contains relatively high levels of total phenolics and flavonoids and that flavonoid isolates from this plant exhibit inhibitory activity against α-glucosidase and α-amylase (Astutiningsih, 2021; Astutiningsih & Meri, 2025; Bouslamti et al., 2023; Peter et al., 2021). However, the specific compounds responsible for α-amylase inhibitory activity in active subfractions of *A. esculentus* fruit remain insufficiently characterized.

Therefore, this study aimed to identify bioactive compounds from *A. esculentus* fruit that contribute to α-amylase inhibitory activity using a bioassay-guided approach combined with in silico characterization. Methanol extract, fractions, and subfractions were evaluated in vitro for α-amylase inhibition, and the most active subfraction was further characterized using LC–MS. The dominant compounds identified in the active subfraction were then assessed through molecular docking and ADMET prediction to support interpretation of their potential as α-amylase inhibitors.

2. METHODS

2.1. Plant Material and Extract Preparation

Fresh fruits of *Abelmoschus esculentus* L. were obtained from a plantation in Toroh, Purwodadi, Central Java, Indonesia. The plant material was authenticated at the Biology Laboratory of Sekolah Tinggi Ilmu Farmasi Yayasan Pharmasi Semarang, and the authentication certificate was issued under reference number 041/EL-AFM/IV/2025. The fruits were washed, dried using in a dryer, and ground into powder. The powdered simplicia was extracted with methanol (Bratachem, Indonesia) at a sample-to-solvent ratio of 1:5 using the maceration method for 3 days. The macerate was filtered, and the solvent was removed using a rotary evaporator until a thick methanol extract was obtained (Astutiningsih & Anggraeny, 2023).

2.2. Fractionation of *A. esculentus* Fruit Extract

The concentrated methanol extract was fractionated successively using *n*-hexane, ethyl acetate, *n*-butanol, and water. A total of 25 g of thick extract was dissolved in 100 mL of distilled water and partitioned with 100 mL of *n*-hexane (Merck, Darmstadt, Germany). Partitioning was repeated until the *n*-hexane phase became clear. The remaining aqueous phase was then partitioned successively with 100 mL of ethyl acetate (Merck, Darmstadt, Germany) and 100 mL of *n*-butanol (Merck, Darmstadt, Germany), with each solvent used repeatedly until the organic phase became clear. The *n*-hexane, ethyl acetate, *n*-butanol, and water fractions were concentrated using a rotary evaporator until thick fractions were obtained (Astutiningsih, 2021).

2.3. Qualitative Phytochemical Screening

Qualitative phytochemical screening was performed on each fraction to detect major secondary metabolite groups, including alkaloids, flavonoids, saponins, phenolic compounds, and tannins. The screening was conducted using standard colorimetric, precipitation, and thin-layer chromatography (TLC) methods. Alkaloids were identified using precipitating reagents, including Dragendorff's, Mayer's, and Bouchardat's reagents, followed by TLC using silica gel GF254 as the stationary phase, ethyl acetate:methanol:water as the mobile phase, and Dragendorff's reagent as the visualization reagent (Hanani, 2015). Flavonoids were identified using Mg powder, concentrated HCl, and amyl alcohol, followed by TLC using silica gel GF254 as the stationary phase, n-butanol:acetic acid:water (4:1:5) as the mobile phase, and ammonia vapor as the visualization reagent (Hanani, 2015). Saponins were identified using the foam test, followed by TLC using silica gel GF254 as the stationary phase, chloroform:methanol:water (64:50:10) as the mobile phase, and anisaldehyde–H_2SO_4 as the visualization reagent (Hanani, 2015). Phenolic compounds were identified using 1% $FeCl_3$ solution, followed by TLC using silica gel GF254 as the stationary phase, methanol:water (6:4) as the mobile phase, and 5% $FeCl_3$ solution as the visualization reagent (Indrayani, 2015). Tannins were

identified using NaCl and gelatin solutions, followed by TLC using silica gel GF254 as the stationary phase, methanol:water (6:4) as the mobile phase, and 5% $FeCl_3$ solution as the visualization reagent (Hanani, 2015).

2.4. α-Amylase Inhibitory Activity Assay

The α-amylase inhibitory activity assay was performed using the 3,5-dinitrosalicylic acid method with a 96-well UV-transparent microplate, following previously reported procedures with modifications (Etsassala et al., 2020; Magaji et al., 2020). Preliminary optimization was performed before the assay. A plate map was prepared in Microsoft Excel to identify each well.

A 25-µL aliquot of substrate was added to wells 1, 3, 5, 7, 9, and 11, followed by 50 µL of sample or positive control and 50 µL of phosphate buffer at pH 6.8. The solution was incubated at 37 °C for 20 min. Subsequently, 25 µL of α-amylase enzyme solution (2 U/mL) was pipetted into wells 2, 3, 5, 7, 9, and 11. The solution was reincubated at 37 °C for 30 min. Then, 100 µL of DNS reagent was added to wells 1, 3, 5, 7, 9, and 11. The microplate was placed in an oven at 100 °C for 10 min. Absorbance was measured at 540 nm using a multimode reader (Astutiningsih, 2021).

2.5. Separation of the Active Fraction by Vacuum Column Chromatography (KVC)

The ethyl acetate fraction, which showed the strongest α-amylase inhibitory activity, was further separated using vacuum column chromatography. The fraction was separated by 2 grams using a KVC with diameter of 5 cm and filled with silica gel GF 254 for TLC as much as 30 grams. Elution was performed using a gradient mobile phase, starting from *n*-hexane 100%; *n*-hexane : ethyl acetate (8:2); *n*-hexane: ethyl acetate (6:4); *n*-hexane : ethyl acetate (4:6); *n*-hexane : ethyl acetate (2:8); ethyl acetate 100%; ethyl acetate: methanol (8:2); ethyl acetate: methanol (6:4); ethyl acetate: methanol (4:6); ethyl acetate: methanol (2:8); ending with 100% methanol Each mobile phase 100 mL until 11 subfraction were identified by TLC method with the stationary phase of silica gel GF 254 and mobile phase Toluen: Ethyl acetate: Formic acid (5:4:0.2). Profiles were observed under (A) UV light at 254 nm, (B) UV light at 366 nm, and (C) ammonia vapor visualization. Subfraction with similar chromatographic profiles based on thin-layer chromatography were combined into subfractions. The combined subfractions were concentrated and subsequently evaluated for α-amylase inhibitory activity (Astutiningsih, 2021).

2.6. Identification of the Most Active Subfraction

The most active subfraction was characterized using UV–Vis spectrophotometry (Shimadzu UV-1700, Japan), FTIR spectroscopy (Agilent Cary 630, USA), and LC–MS analysis (Waters, USA). UV–Vis spectrophotometry was used to observe the absorption spectrum of the subfraction, whereas FTIR spectroscopy was used to identify functional groups. LC–MS analysis was performed at Universitas Padjadjaran, Bandung, Indonesia, to identify the dominant compounds in the active subfraction.

The LC–MS system used was an Acquity UPLC H-Class system (Waters), coupled with a Xevo TQ-S Micro mass spectrometer (Waters). The analysis was performed at a temperature 40^0C and electrospray temperature at 500^0C, with a capillary voltage of 3.0 kV and a cone voltage of 30 V. Full-scan mode was performed over an m/z range of 50–1200. Spectral interpretation was performed using MassLynx v4.2 without spectral libraries. The resulting chromatograms and mass spectral data were used to predict the compound composition of the active subfraction.

2.7. In Silico Molecular Docking of Dominant Compounds as α-Amylase Inhibitors

Molecular docking was performed to evaluate the potential interactions between compounds identified in the active subfraction and the α-amylase enzyme. The crystal structure of α-amylase was obtained from the Protein Data Bank. Ligand structures were prepared in two-dimensional form and converted for docking analysis. Docking simulations were performed using AutoDockTools and AutoDock with the Lamarckian Genetic Algorithm. The docking parameters included 2,500,000 maximum energy evaluations, a population size of 150, a mutation rate of 0.02, a crossover rate of 0.80, and 100 simulation runs.

In the molecular docking simulation, receptor proteins were prepared by removing ligands and water molecules from the active site using BIOVIA Discovery Studio 2021 software. Polar hydrogens were then added, Kollman charges were assigned, and the receptor files were prepared using AutoDockTools. The grid box coordinates were placed at the ligand-binding site. The grid box was prepared to cover all macromolecular residues involved in ligand binding, with a grid box size of 40 × 40 × 40. The natural ligand used was acarbose, which was obtained from PubChem.

The docking method was validated by re-docking the native ligand into the active site of α-amylase. The method was considered acceptable when the root mean square deviation value was <2 Å. Docking results were analyzed based on binding energy, inhibition constant, and ligand interactions with amino acid residues (Radan et al., 2024; Riyaphan et al., 2021).

2.8. Drug-Likeness and ADMET Prediction

The dominant compounds with favorable docking results were further evaluated for drug-likeness and pharmacokinetic properties. Lipinski's rule of five was used to assess molecular weight, lipophilicity, hydrogen bond donors, and hydrogen bond acceptors. ADMET-related parameters, including gastrointestinal absorption, blood–brain barrier permeability, cytochrome P450 interaction, skin permeability, clearance, AMES toxicity, and hepatotoxicity, were predicted using SwissADME and pkCSM. SwissADME was accessed via its webserver (http://www.swissadme.ch/) in [October, 2025], and pkCSM was accessed via its webserver (http://biosig.unimelb.edu.au/pkcsm/) in [October, 2025]. As both tools are web-based platforms without

fixed version numbers, the access date has been provided to ensure reproducibility.

2.9. Statistical Analysis

All experimental data were expressed as mean ± standard deviation. The percentage of α-amylase inhibition was calculated from the absorbance values of the control and sample groups. The IC_{50} value of the methanol extract was determined from the concentration–response curve using regression analysis. Differences in α-amylase inhibitory activity among fractions and subfractions were analyzed using one-way analysis of variance. Statistical significance was set at $p < 0.05$. The quantitative test was obtained from absorbance results data calculated as %inhibition of the α-amylase inhibition activity, then statistically analyzed using SPSS version 26. Molecular docking results were reported as binding energy, inhibition constant, and amino acid interactions, while ADMET and Lipinski parameters were interpreted descriptively.

3. RESULTS AND DISCUSSION

3.1. Extraction Yield and Fractionation Profile

The methanol extraction of dried *Abelmoschus esculentus* fruit produced a concentrated extract with a yield of 31.42%. This result indicates that methanol was able to extract a substantial proportion of polar and semi-polar constituents from the fruit powder. However, extraction yield alone does not necessarily indicate biological activity; therefore, fractionation was performed to separate the extract into fractions with different polarity profiles.

Liquid–liquid fractionation of 100 g of crude methanol extract produced four fractions: *n*-hexane, ethyl acetate, *n*-butanol, and water. The yield of each fraction is presented in **Table 1**. The water fraction showed the highest yield, followed by the *n*-hexane, *n*-butanol, and ethyl acetate fractions. This distribution suggests that the crude methanol extract contained a considerable amount of polar constituents, while nonpolar and semi-polar compounds were also present in measurable amounts.

Table 1. Yield of *A. esculentus* Fruit Fractions

No.	Fraction	Yield (%)
1	n-Hexane	25.87
2	Ethyl acetate	19.34
3	n-Butanol	22.82
4	Water	30.81

Note: Fraction yields were calculated from 100 g of crude methanol extract.

Although the ethyl acetate fraction produced a lower yield than the water and *n*-hexane fractions, this fraction was expected to contain semi-polar compounds such as phenolics and flavonoids. Previous studies have reported that *A. esculentus* fruit contains phenolic and flavonoid compounds, including quercetin and related derivatives, which may contribute to enzyme inhibitory activity (Agregán et al., 2023; Astutiningsih, 2021; Sun & Shahrajabian, 2023). Therefore, further biological testing was required to determine which fraction contained the most active α-amylase inhibitory constituents.

3.2. α-Amylase Inhibitory Activity of Extract and Fractions

The α-amylase inhibitory activity of the methanol extract was first evaluated using the IC_{50} parameter, with acarbose as the positive control. As shown in **Table 2**, the methanol extract showed an IC_{50} value of 116.4031 µg/mL, whereas acarbose showed an IC_{50} value of 43.99 µg/mL. Because a lower IC_{50} value indicates stronger inhibitory activity, the methanol extract was less active than acarbose but still showed measurable α-amylase inhibitory potential.

Table 2. IC_{50} Values of α-Amylase Inhibition

Sample	IC_{50}
Acarbose	43.99 µg/mL
A. esculentus fruit extract	116.4031 µg/mL

Note: IC_{50} represents the concentration required to inhibit 50% of α-amylase activity.

Fraction testing showed that α-amylase inhibitory activity differed significantly among the fractions and positive control (**Figure 1**). Acarbose produced the highest inhibition, at 74.0151 ± 3.2502%, and differed significantly from all fractions based on Tukey's post hoc test ($p < 0.05$). Among the fractions, the ethyl acetate fraction showed the strongest inhibitory activity, with 66.5813 ± 2.6941%, and was significantly higher than the *n*-butanol fraction (58.5491 ± 2.4269%) and water fraction (54.9929 ± 5.0016%). The *n*-butanol and water fractions did not differ significantly from each other, whereas the *n*-hexane fraction showed the lowest activity, indicating that nonpolar constituents did not contribute substantially to α-amylase inhibition under the assay conditions.

The stronger activity of the ethyl acetate fraction suggests that the compounds responsible for α-amylase inhibition were more likely concentrated in the semi-polar fraction. This result is consistent with previous reports that ethyl acetate fractions of *A. esculentus* fruit contain relatively high levels of phenolic and flavonoid compounds (Astutiningsih & Anggraeny, 2023; Peter et al., 2021). These findings supported the selection of the ethyl acetate fraction for further subfractionation.

3.3. Subfractionation and Thin-Layer Chromatography Profile

The ethyl acetate fraction was further separated using vacuum liquid chromatography with silica gel GF254 as the stationary phase and a gradient mobile phase system. Separation produced eleven eluate fractions, which were grouped into three combined subfractions based on similarity of thin-layer chromatography profiles. The TLC profiles observed under UV 254 nm, UV 366 nm, and ammonia vapor are shown in **Figure 2**. The TLC profile showed that the combined subfractions differed in polarity and compound distribution. Subfractions obtained from lower-polarity eluents showed spots corresponding to relatively less polar constituents, whereas later eluents containing methanol indicated

the presence of more polar compounds. These differences supported the grouping of eluates into subfractions for further α-amylase inhibitory testing.

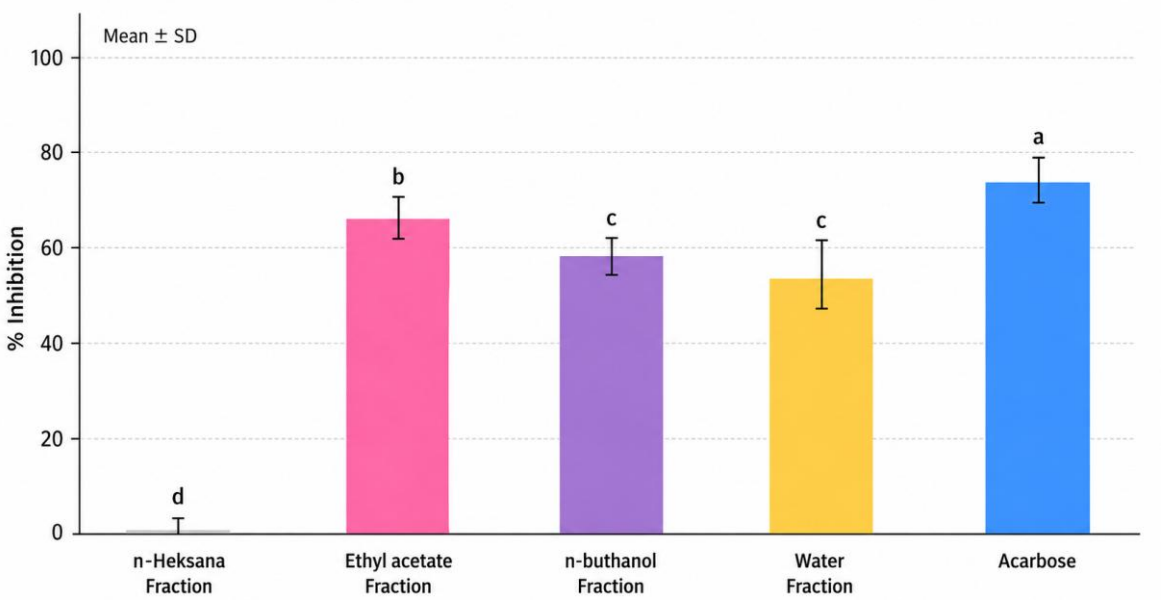

Figure 1. Percentage inhibition of α-amylase activity by acarbose and *A. esculentus* fruit fractions. Data are presented as mean ± SD. Different lowercase letters indicate significant differences according to Tukey's post hoc test ($p < 0.05$).

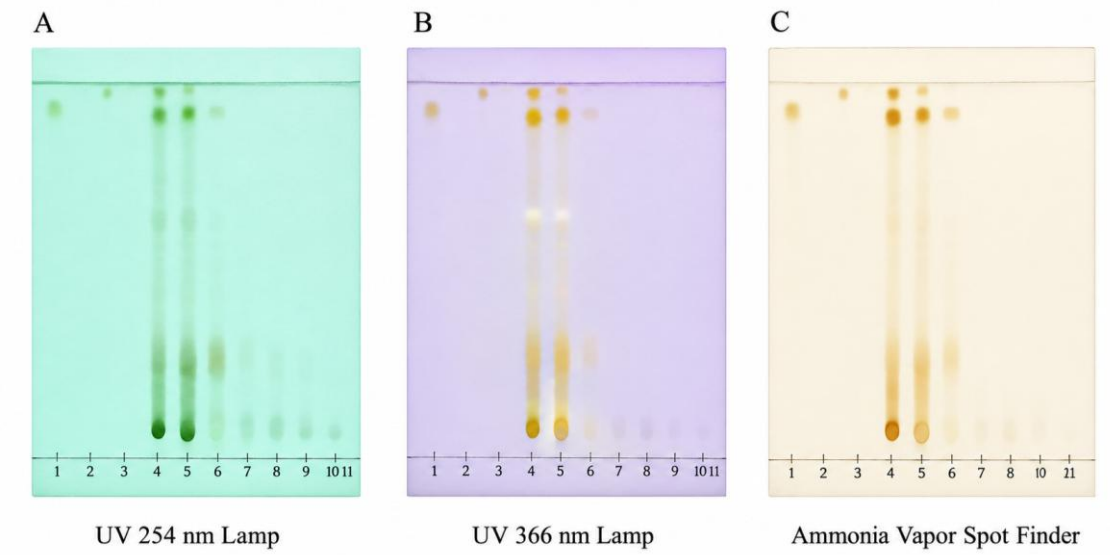

Figure 2. Thin-layer chromatographic profiles of subfractions from the ethyl acetate fraction of *A. esculentus* fruit. Profiles were observed under (A) UV light at 254 nm, (B) UV light at 366 nm, and (C) ammonia vapor visualization. Lane 1 = 100% *n*-hexane; lane 2 = *n*-hexane:ethyl acetate (8:2, v/v); lane 3 = *n*-hexane:ethyl acetate (6:4, v/v); lane 4 = *n*-hexane:ethyl acetate (4:6, v/v); lane 5 = *n*-hexane:ethyl acetate (2:8, v/v); lane 6 = 100% ethyl acetate; lane 7 = ethyl acetate:methanol (8:2, v/v); lane 8 = ethyl acetate:methanol (6:4, v/v); lane 9 = ethyl acetate:methanol (4:6, v/v); lane 10 = ethyl acetate:methanol (2:8, v/v); lane 11 = 100% methanol.

3.4. α-Amylase Inhibitory Activity of Subfractions

Subfraction testing showed that α-amylase inhibitory activity was concentrated mainly in subfraction 2. As shown in Figure 3, subfraction 2 produced the highest inhibition value, 74.2634 ± 4.7091%, followed by subfraction 3 with 59.4281 ± 2.0850% and subfraction 1 with 24.0901 ± 4.5147%. This result indicates that the active compounds were enriched during subfractionation of the ethyl acetate fraction. The strong inhibitory activity of subfraction 2 suggests that medium-polar constituents may play a major role in α-amylase inhibition. The inhibition value of subfraction 2 was close to that of acarbose in the fraction assay, indicating that further chemical characterization of this subfraction was justified. Therefore, subfraction 2 was selected for compound identification using LC–MS and subsequent in silico evaluation.

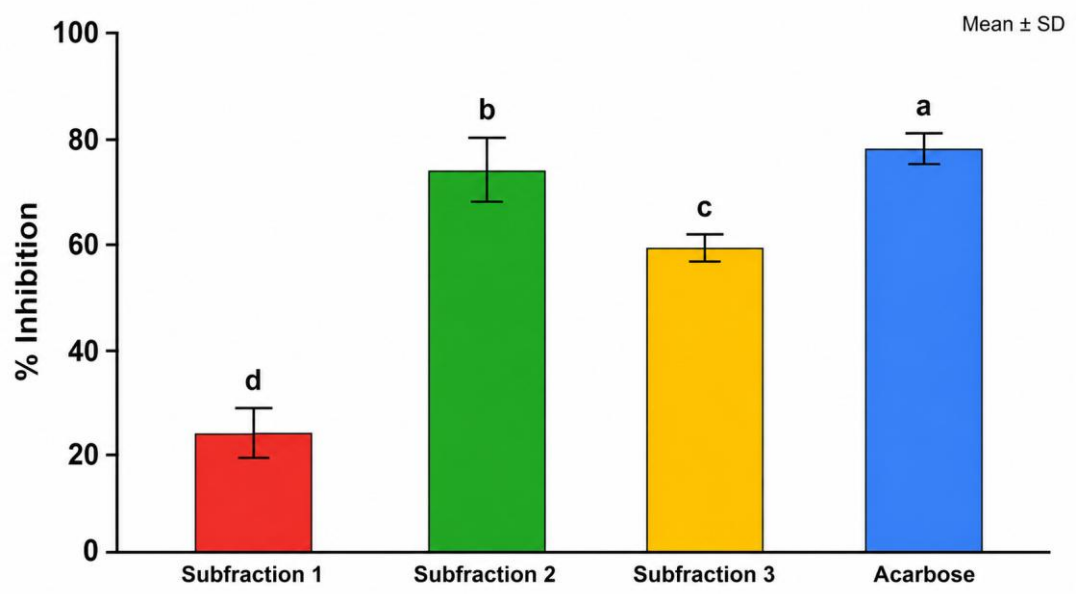

Figure 3. α-Amylase inhibitory activity of *A. esculentus* fruit subfractions and acarbose. Data are presented as mean ± SD. Different lowercase letters indicate significant differences according to Tukey's post hoc test ($p < 0.05$).

3.5. LC–MS Identification of Compounds in the Active Subfraction

LC–MS analysis of subfraction 2 identified nine tentative compounds with different retention times, molecular formulas, and relative compositions (**Table 3**). The largest relative composition was observed for 3-hydroxy-2,3-dihydroimidazo[1,5-a]pyridin-8(5H)-one-5-β-glucopyranoside, followed by Coumaroyl tyramine, quercetin, fraxidin, 3-(4-hydroxy-3-methoxyphenyl)-N-[2-(4-hydroxyphenyl)ethyl]prop-2-enimidic acid, 2-hydroxy-7-methoxycadalene, 2-methoxy-4-(2-phenylethyl)phenol, homovanillic acid, and scopoletin. The compounds identified in subfraction 2 were mainly phenolic, flavonoid, terpenoid, and phenol amide-related constituents. These compound classes are relevant to α-amylase inhibitory activity because phenolics and flavonoids may interact with digestive enzymes through hydrogen bonding and hydrophobic interactions, thereby reducing enzyme activity (Bouslamti et al., 2023; Riyaphan et al., 2021). Nevertheless, LC–MS identification alone does not confirm which individual compound is primarily responsible for the observed inhibition; therefore, molecular docking was used as a complementary predictive approach.

Table 3. LC–MS Identification of Compounds in Subfraction 2 of *A. esculentus* Fruit

No.	Rt (min)	Parent ion (m/z)	Molecular weight	Molecular formula	Compound name	Composition (%)	Classification
1	6.47	246.0879	245.23	$C_{12}H_{11}N_3O_3$	3-Hydroxy-2,3-dihydroimidazo[1,5-a]pyridin-8(5H)-one-5-β-glucopyranoside (Kehinde et al., 2022)	42.46	Flavonoid
2	6.71	193.0501	192.17	$C_{10}H_8O_4$	Scopoletin (Ahmed et al., 2017)	1.51	Flavonoid
3	6.81	223.0606	222.37	$C_{11}H_{10}O_5$	Fraxidin (Kasmi et al., 2021)	6.34	Phenolic
4	7.04	183.17	182.20	$C_{10}H_{12}O_4$	Homovanillic acid (Aguilar-Camacho et al., 2024)	1.67	Phenolic acid
5	7.17	314.1392	313.35	$C_{18}H_{19}NO_4$	3-(4-Hydroxy-3-methoxyphenyl)-N-[2-(4-hydroxyphenyl)ethyl]prop-2-enimidic acid (Højmark, 2020)	4.77	Phenolic acid
6	7.58	303.0505	302.24	$C_{15}H_{10}O_7$	Quercetin (Kehinde et al., 2022)	13.23	Flavonoid
7	8.24	245.1542	244.33	$C_{16}H_{20}O_2$	2-Hydroxy-7-methoxycadalene (Stipanovic et al., 1981)	4.33	Terpenoid
8	8.41	227.0188	228.00	$C_{15}H_{16}O_2$	2-Methoxy-4-(2-phenylethyl)phenol (Schwab et al., 1990)	.14	Phenol
9	9.06	271.33	270.45	$C_{17}H_{34}O_2$	Coumaroyl tyramine (Hu et al., 2024)	19.18	Phenol

Note: Compound identification was based on LC–MS interpretation and should be considered tentative unless confirmed using authentic standards or additional structural elucidation.

3.6. Molecular Docking Validation and Binding Interaction Analysis

The molecular docking procedure was validated by re-docking the native ligand into the α-amylase binding site. The redocking process produced an RMSD value of 1.96 Å, which is within the generally acceptable threshold of less than 2 Å. This result indicates that the docking method was suitable for predicting ligand interactions with the α-amylase binding site. The redocking produced a binding energy of −3.14 kcal/mol and an inhibition constant of 5.02 mM. The 2D visualization of the docking interaction is shown in **Figure 4**.

Molecular docking of the nine LC–MS-identified compounds produced binding energies ranging from −4.92 to −5.82 kcal/mol (**Table 4**). The compound 3-(4-hydroxy-3-methoxyphenyl)-N-[2-(4-hydroxyphenyl)ethyl]prop-2-enimidic acid showed the most negative binding energy, whereas several other compounds showed interaction patterns involving important amino acid residues, including Asn279, Gly283, Tyr276, Glu272, Trp284, and Lys261. These residues were also involved in interactions with the reference ligand, suggesting that selected compounds from subfraction 2 may bind within or near the α-amylase active region.

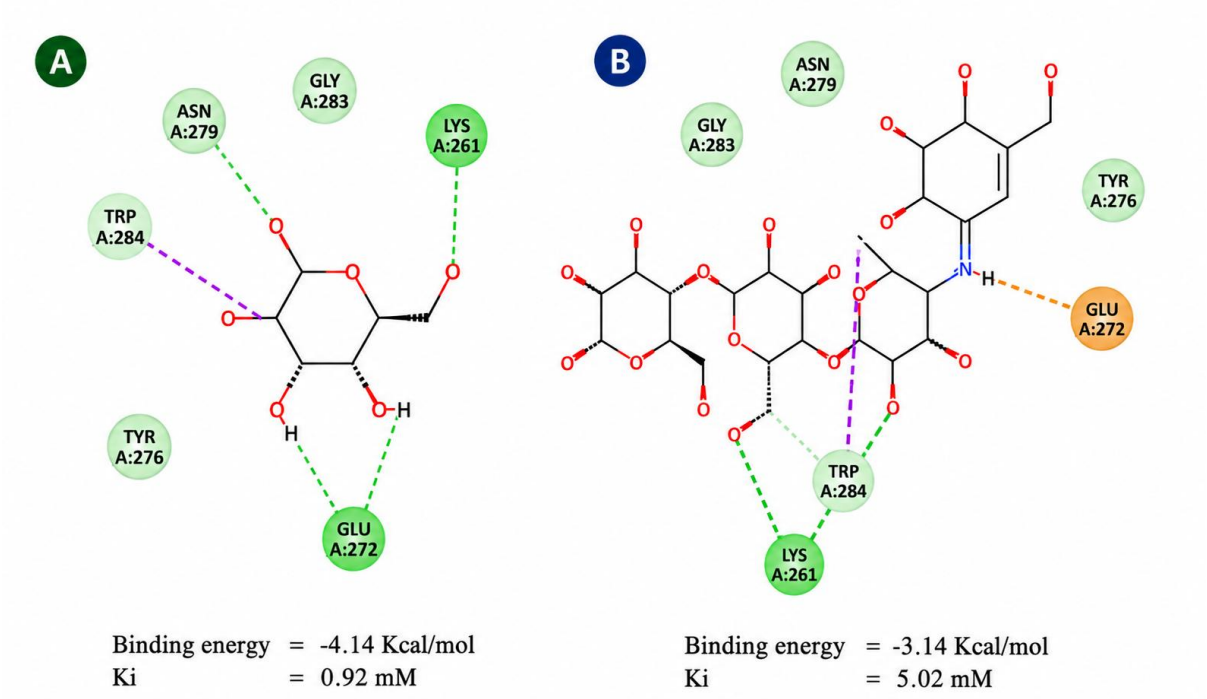

Figure 4. Two-dimensional visualization of docking interactions between α-amylase and the reference ligand or positive control. (A) Natural ligand interaction; (B) positive control interaction.

Table 4. Molecular Docking Results of LC–MS-Identified Compounds against α-Amylase Using AutoDock4

No.	Compound	Binding energy (kcal/mol)	Inhibition constant	Amino acid interactions
1	3-Hydroxy-2,3-dihydroimidazo[1,5-a]pyridin-8(5H)-one-5-β-glucopyranoside	−4.99 ± 0.00	220.27 ± 0.06	Glu272, Trp284
2	Scopoletin	−5.09 ± 0.00	187.77 ± 0.47	Asn279, Tyr276, Trp284, Lys261
3	Fraxidin	−4.92 ± 0.00	248.01 ± 0.80	Asn279, Tyr276, Glu272, Trp284, Lys261
4	Homovanillic acid	−5.59 ± 0.01	81.90 ± 3.20	Gly283, Asn279, Tyr276, Glu272, Trp284, Lys261
5	3-(4-Hydroxy-3-methoxyphenyl)-N-[2-(4-hydroxyphenyl)ethyl]prop-2-enimidic acid	−5.82 ± 0.06	54.39 ± 5.38	Glu272, Trp284, Tyr276
6	Quercetin	−5.67 ± 0.33	96.14 ± 3.04	Asn279, Gly283, Tyr276, Glu272, Trp284, Lys261
7	2-Hydroxy-7-methoxycadalene	−5.74 ± 0.00	61.79 ± 0.38	Asn279, Gly283, Tyr276, Glu272, Trp284, Lys261
8	2-Methoxy-4-(2-phenylethyl)phenol	−5.27 ± 0.01	137.49 ± 3.33	Glu272, Trp284
9	Coumaroyl tyramine	−5.71 ± 0.02	65.63 ± 2.79	Asn279, Asp412, Gly283, Gly413, Tyr276, Glu272, Trp409, Ser275, Lys278

Note: The unit of the inhibition constant should be confirmed by the authors based on the AutoDock output.

The docking results suggest that several compounds in subfraction 2 may contribute to α-amylase inhibition. Although compound 5 showed the most negative binding energy, four compounds showed favorable binding profiles and shared several amino acid interactions with the reference ligand: homovanillic acid, quercetin, 2-hydroxy-7-methoxycadalene, and Coumaroyl tyramine. These compounds may contribute to the in vitro α-amylase inhibitory activity observed for subfraction 2. However, docking results represent computational predictions and cannot independently confirm biological activity. Therefore, the in silico findings should be interpreted as supportive evidence that complements the in vitro bioassay results.

3.7. Drug-Likeness and ADMET Prediction

The four selected compounds were further evaluated using Lipinski and ADMET prediction parameters (**Table 5**). The analysis showed that all four compounds were reported to meet Lipinski's rule of five with no violations. These results suggest that the selected compounds have preliminary physicochemical properties compatible with oral drug-likeness.

Table 5. Lipinski and ADMET Prediction of Selected Compounds

Parameter	Homovanillic acid	Quercetin	2-Hydroxy-7-methoxycadalene	Coumaroyl tyramine
Formula	$C_9H_{10}O_4$	$C_{15}H_{10}O_7$	$C_{16}H_{20}O_2$	$C_{17}H_{34}O_2$
Molecular weight	182.17 g/mol	302.24 g/mol	244.33 g/mol	270.45 g/mol
H-bond acceptors	4	7	2	2
H-bond donors	2	5	1	0
TPSA	66.75 Å^2	131.36 Å^2	29.46 Å^2	26.30 Å^2
Consensus log P	0.88	1.23	4.03	5.54
GI absorption	High	High	High	High
BBB permeant	No	Yes	Yes	Yes
CYP2C9 inhibition	No	No	No	No
Log Kp	−7.18	−7.05	−4.50	−6.10
Lipinski	Yes, 0 violation	Yes, 0 violation	Yes, 0 violation	Yes, 0 violation
Total clearance	0.246	0.407	0.188	0.265
AMES toxicity	No	No	Yes	No
Hepatotoxicity	No	No	No	No

Note: ADMET values are computational predictions and should be verified experimentally before pharmacological development.

Homovanillic acid and quercetin showed relatively lower lipophilicity, while 2-hydroxy-7-methoxycadalene and Coumaroyl tyramine showed higher lipophilicity values. The predicted high gastrointestinal absorption for all four compounds suggests potential oral absorbability. Homovanillic acid was not predicted to cross the blood–brain barrier, whereas the other three compounds were predicted to be BBB-permeant. Because α-amylase acts in the gastrointestinal tract, BBB permeability is not necessarily required for the intended mechanism and may be more relevant for safety considerations.

The ADMET prediction also showed that 2-hydroxy-7-methoxycadalene was predicted to have AMES toxicity, whereas the other three compounds were not. This finding indicates that, although 2-hydroxy-7-methoxycadalene showed favorable docking interactions, its safety profile requires further evaluation. Overall, the ADMET results support the preliminary selection of homovanillic acid, quercetin, 2-hydroxy-7-methoxycadalene, and Coumaroyl tyramine as candidate compounds, but additional experimental validation is necessary.

The combined in vitro and in silico findings indicate that subfraction 2 of *A. esculentus* fruit contains compounds with potential α-amylase inhibitory activity. The in vitro assay showed that subfraction 2 produced 74.2634 ± 4.7091% inhibition, while molecular docking suggested that several identified compounds may interact with amino acid residues in the α-amylase binding region. These results support the use of a bioassay-guided strategy to prioritize active subfractions and candidate compounds. However, the findings remain preliminary because LC–MS identification was tentative, molecular docking was predictive, and no enzyme kinetic study or compound isolation confirmation was performed.

4. CONCLUSION

Subfraction 2 of *Abelmoschus esculentus* fruit showed the strongest α-amylase inhibitory activity, with an inhibition value of 74.2634 ± 4.7091%, indicating that the active constituents were concentrated during bioassay-guided fractionation. LC–MS analysis tentatively identified nine compounds in this subfraction, while molecular docking suggested that four compounds—2-hydroxy-7-methoxycadalene, Coumaroyl tyramine, homovanillic acid, and quercetin—had favorable binding profiles and amino acid interactions with α-amylase. These findings indicate that *A. esculentus* fruit is a potential source of α-amylase inhibitory compounds. However, further studies involving compound isolation, structural confirmation, enzyme kinetic analysis, and in vivo evaluation are required to validate its antidiabetic potential.

AUTHOR CONTRIBUTIONS

Conceptualization, C.A. and S.R.; methodology, C.A. and S.R.; software, N.D.S.; validation, C.A. and S.R.; formal analysis, S.R.; investigation, S.R. and N.D.S.; resources, C.A.; data curation, S.R.; writing—original draft preparation, N.D.S. and S.R.; writing—review and editing, C.A., S.R., and

N.D.S.; visualization, C.A. and N.D.S.; supervision, C.A.; project administration, C.A. and S.R.; funding acquisition, C.A. All authors have read and agreed to the published version of the manuscript.

INSTITUTIONAL REVIEW BOARD STATEMENT

Not applicable.

INFORMED CONSENT STATEMENT

Not applicable.

DATA AVAILABILITY STATEMENT

Data supporting the findings of this study are available upon reasonable request from the corresponding author.

FUNDING

This research was funded by Yayasan Pharmasi Semarang, grant number No. 03/LPPM/LK-TM/PDL/VI/2024.

ACKNOWLEDGMENT

The authors gratefully acknowledge Yayasan Pharmasi Semarang and Sekolah Tinggi Ilmu Farmasi Yayasan Pharmasi Semarang for providing financial support and research facilities for this study.

CONFLICTS OF INTEREST

The authors declare no conflict of interest.

ROLE OF FUNDERS

The funders had no role in the design of the study; in the collection, analyses, or interpretation of data; in the writing of the manuscript; or in the decision to publish the results.

DECLARATION OF GENERATIVE ARTIFICIAL INTELLIGENCE (AI) USE

During the preparation of this manuscript, the authors used ChatGPT (OpenAI) to assist in improving the clarity, structure, grammar, and readability of the text. After using this tool, the authors thoroughly reviewed, edited, and verified the entire content to ensure that it accurately represents their own ideas, data, analyses, and interpretations. The authors take full responsibility for the integrity, accuracy, and originality of the published work.

REFERENCES

Agregán, R., Pateiro, M., Bohrer, B. M., Shariati, M. A., Nawaz, A., Gohari, G., & Lorenzo, J. M. (2023). Biological activity and development of functional foods fortified with okra (*Abelmoschus esculentus*). *Critical Reviews in Food Science and Nutrition, 63*(23), 6018–6033. https://doi.org/10.1080/10408398.2022.2026874

Aguilar-Camacho, M., Gómez-Sánchez, C. E., Cruz-Mendívil, A., Luna-Vital, D. A., Guerrero-Analco, J. A., Monribot-Villanueva, J. L., & Gutiérrez-Uribe, J. A. (2024). Untargeted metabolomic analysis of *Randia echinocarpa* cell cultures treated with L-tyrosine. *Plant Cell, Tissue and Organ Culture, 158*(1), Article 14. https://doi.org/10.1007/s11240-024-02808-3

Ahmad, S., Ali, M., Ali, J., Khan, A., Khan, S., Ullah, Z., Rafiullah, & Hussain, S. (2025). Factors influencing adherence to recommended treatment among individuals with type 2 diabetes: A cross-sectional study from tertiary hospital Swat, Pakistan. *Frontier in Medical and Health Research, 3*(5), 507–519. https://doi.org/10.5281/zenodo.15854344

Ahmed, O. H., Hamad, M. N., & Jaafar, N. S. (2017). Phytochemical investigation of *Chenopodium murale* (family: Chenopodiaceae) cultivated in Iraq, isolation and identification of scopoletin and gallic acid. *Asian Journal of Pharmaceutical and Clinical Research, 10*(11), 70–77. https://doi.org/10.22159/ajpcr.2017.v10i11.20504

Astutiningsih, C. (2021). Isolation and inhibition test of quercetin compound from okra fruit (*Abelmoschus esculentus* L.). *Jurnal Farmasi Sains dan Praktis, 7*(3), 356–364. https://doi.org/10.31603/pharmacy.v7i3.6203

Astutiningsih, C., & Anggraeny, E. N. (2023). Penentuan fenolik total, flavonoid total, aktivitas antioksidan dan nilai SPF fraksi buah okra (*Abelmoschus esculentus* L.). *Cendekia Eksakta, 8*(1). https://doi.org/10.31942/ce.v8i1.8260

Astutiningsih, C., & Meri, M. (2025). Potential of flavonoid isolate from okra fruit (*Abelmoschus esculentus* L.) as antidiabetic and antilipase agent in vitro and in silico. *Jurnal Farmasi Sains dan Terapan (Journal of Pharmacy Science and Practice), 12*(1), 34–46. https://doi.org/10.33508/jfst.v12i1.6053

Bouslamti, M., Loukili, E. H., Elrherabi, A., El Moussaoui, A., Chebaibi, M., Bencheikh, N., Nafidi, H.-A., Bin Jardan, Y. A., Bourhia, M., Bnouham, M., Lyoussi, B., & Benjelloun, A. S. (2023). Phenolic profile, inhibition of α-amylase and α-glucosidase enzymes, and antioxidant properties of *Solanum elaeagnifolium* Cav. (Solanaceae): In vitro and in silico investigations. *Processes, 11*(5), Article 1384. https://doi.org/10.3390/pr11051384

Dong, Y., Sui, L., Yang, F., Ren, X., Xing, Y., & Xiu, Z. (2022). Reducing the intestinal side effects of acarbose by baicalein through the regulation of gut microbiota: An in vitro study. *Food Chemistry, 394*, Article 133561. https://doi.org/10.1016/j.foodchem.2022.133561

Durazzo, A., Lucarini, M., Novellino, E., Souto, E. B., Daliu, P., & Santini, A. (2018). *Abelmoschus esculentus* (L.): Bioactive components' beneficial properties—Focused on antidiabetic role—for sustainable health applications. *Molecules, 24*(1), Article 38. https://doi.org/10.3390/molecules24010038

Etsassala, N. G. E. R., Badmus, J. A., Marnewick, J. L., Iwuoha, E. I., Nchu, F., & Hussein, A. A. (2020). Alpha-glucosidase and alpha-amylase inhibitory activities, molecular docking, and antioxidant capacities of *Salvia aurita* constituents. *Antioxidants, 9*(11), Article 1149. https://doi.org/10.3390/antiox9111149

Ghosh, A., Maheshwari, V., & Basu, S. (2025). Self-care practices and their determinants among older adults with diabetes and hypertension in India: Evidence from a national survey. *International Journal of Diabetes in Developing Countries*. https://doi.org/10.1007/s13410-025-01541-7

Hafeez, M., Hassan, S. M., Mughal, S. S., Munir, M., & Khan, M. K. (2020). Antioxidant, antimicrobial and cytotoxic potential of *Abelmoschus esculentus*. *Chemical and Biomolecular Engineering, 5*(4), 69–79. https://doi.org/10.11648/j.cbe.20200504.11

Hanani, E. 2015. *Analisis Fitokimia*. Buku Kedokteran EGC, Jakarta.

Herowati, R., Puradewa, L., Herdianty, J., & Widodo, G. P. (2020). Antidiabetic activity of okra fruit (*Abelmoschus esculentus* (L.) Moench) extract and fractions in two conditions of diabetic rats. *Indonesian Journal of Pharmacy, 31*(1), 27–34. https://doi.org/10.14499/indonesianjpharm31iss1pp27

Højmark, L. A. B. (2020). *Analysis of the marine sponge Pachymatisma normani* [Master's thesis, University of Bergen].

Hu, W., Nie, Y., Huang, L., & Qian, D. (2024). Contribution of phenolamides to the quality evaluation in *Lycium* spp. *Journal of Ethnopharmacology, 331*, Article 118220. https://doi.org/10.1016/j.jep.2024.118220

Kasmi, S., Hamdi, A., Atmani-Kilani, D., Debbache-Benaida, N., Jaramillo-Carmona, S., Rodríguez-Arcos, R., Jiménez-Araujo, A., Ayouni, K., Atmani, D., & Guillén-Bejarano, R. (2021). Characterization of phenolic compounds isolated from the *Fraxinus angustifolia* plant and several associated bioactivities. *Journal of Herbal Medicine, 29*, Article 100485. https://doi.org/10.1016/j.hermed.2021.100485

Kehinde, I. O., Olatunji, O. E., & Adegoke, A. (2022). Electrocardiography effects of *Abelmoschus esculentus* fruit extract and its isolated compounds using isolated frog heart perfusion. *World Journal of Advanced Research and Reviews, 14*(2), 104–111. https://doi.org/10.30574/wjarr.2022.14.2.0368

Li, X., Bai, Y., Jin, Z., & Svensson, B. (2022). Food-derived non-phenolic α-amylase and α-glucosidase inhibitors for controlling starch digestion rate and guiding diabetes-friendly recipes. *LWT, 153*, Article 112455. https://doi.org/10.1016/j.lwt.2021.112455

Magaji, U. F., Sacan, O., & Yanardag, R. (2020). Alpha amylase, alpha glucosidase and glycation inhibitory activity of *Moringa oleifera* extracts. *South African Journal of Botany, 128*, 225–230. https://doi.org/10.1016/j.sajb.2019.11.024

Młynarska, E., Czarnik, W., Dzieża, N., Jędraszak, W., Majchrowicz, G., Prusinowski, F., Stabrawa, M., Rysz, J., & Franczyk, B. (2025). Type 2 diabetes mellitus: New pathogenetic mechanisms, treatment and the most important complications. *International Journal of Molecular Sciences, 26*(3), Article 1094. https://doi.org/10.3390/ijms26031094

Oguntibeju, O. O. (2019). Type 2 diabetes mellitus, oxidative stress and inflammation: Examining the links. *International Journal of Physiology, Pathophysiology and Pharmacology, 11*(3), 45–63.

Panighel, G., Ferrarese, I., Lupo, M. G., Sut, S., Dall'Acqua, S., & Ferri, N. (2022). Investigating the in vitro mode of action of okra (*Abelmoschus esculentus*) as hypocholesterolemic, anti-inflammatory, and antioxidant food. *Food Chemistry: Molecular Sciences, 5*, Article 100126. https://doi.org/10.1016/j.fochms.2022.100126

Peter, E. L., Nagendrappa, P. B., Ajayi, C. O., & Sesaazi, C. D. (2021). Total polyphenols and antihyperglycemic activity of aqueous fruits extract of *Abelmoschus esculentus*: Modeling and optimization of extraction conditions. *PLOS ONE, 16*(4), Article e0250405. https://doi.org/10.1371/journal.pone.0250405

Radan, M., Ćujić Nikolić, N., Kuzmanović Nedeljković, S., Mutavski, Z., Krgović, N., Stević, T., Marković, S., Jovanović, A., Živković, J., & Šavikin, K. (2024). Multifunctional pomegranate peel microparticles with health-promoting effects for the sustainable development of novel nutraceuticals and pharmaceuticals. *Plants, 13*(2), Article 281. https://doi.org/10.3390/plants13020281

Rivas, A. M., & Nugent, K. (2021). Hyperglycemia, insulin, and insulin resistance in sepsis. *The American Journal of the Medical Sciences, 361*(3), 297–302. https://doi.org/10.1016/j.amjms.2020.11.007

Riyaphan, J., Pham, D.-C., Leong, M. K., & Weng, C.-F. (2021). In silico approaches to identify polyphenol compounds as α-glucosidase and α-amylase inhibitors against type-II diabetes. *Biomolecules, 11*(12), Article 1877. https://doi.org/10.3390/biom11121877

Schwab, W., Scheller, G., & Schreier, P. (1990). Glycosidically bound aroma components from sour cherry. *Phytochemistry, 29*(2), 607–612. https://doi.org/10.1016/0031-9422(90)85126-Z

Shareef, A. A., Farhan, F. J., & Alriyahee, F. A. A. (2023). Antibacterial activity of silver nanoparticles composed by fruit aqueous extract of *Abelmoschus esculentus* (L.) Moench alone or in combination with antibiotics. *Basrah Journal of Agricultural Sciences, 36*(2), 144–174. https://doi.org/10.37077/25200860.2023.36.2.12

Stipanovic, R. D., Greenblatt, G. A., Beier, R. C., & Bell, A. A. (1981). 2-Hydroxy-7-methoxycadalene: The precursor of lacinilene C 7-methyl ether in *Gossypium*. *Phytochemistry, 20*(4), 729–730. https://doi.org/10.1016/0031-9422(81)85162-X

Sun, W., & Shahrajabian, M. H. (2023). Therapeutic potential of phenolic compounds in medicinal plants—Natural health products for human health. *Molecules, 28*(4), Article 1845. https://doi.org/10.3390/molecules28041845

Ullah, H., Jan, T., Ahmad, B., Nawaz, T., Khan, I., Ahmad, K., Rehman, A. U., Murshed, A., Lu, J., & Ali, A. (2024). Phytochemical profiling and therapeutic potential of *Abelmoschus esculentus* fruit extracts: Insights into antidiabetic potential in in vitro and in vivo experiments. *Journal of Food Quality, 2024*, Article 7096736. https://doi.org/10.1155/2024/7096736

Xiong, B., Zhang, W., Wu, Z., Liu, R., Yang, C.-Y., Hui, A., Huang, X., & Xian, Z. (2021). Preparation, characterization, antioxidant and anti-inflammatory activities of acid-soluble pectin from okra (*Abelmoschus esculentus* L.). *International*

Journal of Biological Macromolecules, 181, 824–834. https://doi.org/10.1016/j.ijbiomac.2021.03.202